Article:

Wang, Q, Lorinczi, P and Glover, PWJ orcid.org/0000-0003-1715-5474 (2020) Oil Production and Reservoir Damage during Miscible CO2 Injection. The Leading Edge, 39 (1). pp. 22-28. ISSN 1070-485X

https://doi.org/10.1190/tle39010022.1

Oil Production and Reservoir Damage during Miscible CO_2 Injection

Qian Wang[1, 2], Piroska Lorinczi[2], Paul W.J. Glover[2]*

1 School of Petroleum Engineering, China University of Petroleum-Beijing, Beijing 102249, China
2 School of Earth and Environment, University of Leeds, Leeds, LS2 9JT, UK
***Correspondence:** p.w.j.glover@leeds.ac.uk

Abstract. The blockage and alteration of wettability in reservoirs caused by asphaltene deposits are serious problems which contribute to poor oil recovery performance during CO_2 injection. Oil production and reservoir damage are both controlled by macroscopic interlayer heterogeneity and microscopic pore-throat structure, and may be optimised by the choice of flooding method. In this work, the residual oil distribution and the permeability decline caused by organic and inorganic precipitation after (i) miscible CO_2 flooding, and (ii) water-alternating-CO_2 (CO_2-WAG) flooding have been studied by carrying out core-flooding experiments on a model heterogeneous 3-layer reservoir. For CO_2, flooding experimental results indicate that the low permeability layers retain a large oil production potential even in the late stages of production, while the permeability decline due to formation damage is larger in the high permeability layer. We found that CO_2-WAG can reduce the influence of heterogeneity on the oil production, but it results in more serious reservoir damage, with permeability decline caused by CO_2–brine–rock interactions becoming significant. In addition, miscible CO_2 flooding has been carried out for rocks with very similar permeabilities but (i) different wettabilities, and (ii) different pore throat microstructures, in order to study the effects of wettability and pore throat microstructure on formation damage. Reservoir rocks with smaller pore throat sizes and more heterogeneous pore-throat microstructures were found to be more sensitive to asphaltene precipitation, with corresponding lower oil recovery and greater decreases in permeability. However, it was found that the degree of water-wetness for cores with larger, more connected pore-throat microstructures became weaker due to asphaltene precipitation to pore surfaces. Decreasing the degree of water-wetness was found to be exacerbated by increases in the sweep volume of injected CO_2 that arise from cores with larger and m better ore connected pore throats. Erosion of water-wetness is a disadvantage for enhancing oil recovery (EOR) operations as asphaltene precipitation prevention and control measures become more necessary.

Introduction

The Chang Qing Oilfield is a typical low-permeability sandstone reservoir located in the Ordos Basin in western China (38°30’09”N, 108°50’37”E). The target reservoir lies at a depth of 2100-2400 m (T_{res}=70±7°C, P_{res}=18±1.5 MPa) and consists of a series of thin layers with different permeability values, separated by shaly baffles. Flooding by the injection of CO_2 is being investigated for both enhanced oil recovery (EOR) and CO_2 storage. It is known that both oil production performance and residual oil distribution are affected by the choice of CO_2 injection method, and that this is especially the case for multi-layer reservoirs with high interlayer heterogeneity (Lei et al., 2016). Flooding with both CO_2 and CO_2-WAG are common EOR strategies which have been widely used in a significant number of oilfields (Han et al., 2014). In addition, the wettability, pore size distribution (Al-Mahrooqi et al., 2003) and pore-throat microstructure (Li et al., 2018) of the rocks are also important factors in determining the distribution of microscopic residual oil during CO_2 injection.

When the fluid pressure reaches a certain value during the CO_2 injection process, changes in composition of the crude oil due to the dissolved CO_2 lead to asphaltene precipitation. The solid asphaltene particles become captured or adsorbed on the pore walls, resulting in blocked pores and pore throats, and can also cause changes of wettability (Al-Maamari et al., 2003). Precipitation of insoluble metal carbonates and the release of clay particles caused by CO_2-brine-rock interactions are also non-negligible factors, which may lead to changes in the petrophysical properties of the reservoir rocks, and which are exhibited as formation damage (Wang et al., 2019). In addition, changes in the rocks' petrophysical properties due to asphaltene precipitation and CO_2-brine-rock interaction are exacerbated by heterogeneity, the choice of the CO_2 injection schemes, as well as the pore-throat microstructure (Wang et al., 2017; Zou et al., 2018). Moreover, the adsorption/desorption of organic molecules to the mineral surfaces in tightly constrained pores is also a factor (Kong et al., 2019; Liu et al., 2018). At present, for strongly heterogeneous, multi-layer and low-permeability sandstone reservoirs, numerical simulation lacks either reliable supporting data or a robust theoretical framework because there has been a lack of corresponding experimental studies on these issues; a lacuna that we are trying to fill with this work.

This work presents two sets of core-flooding experiments which have been carried out at reservoir conditions (70°C, 18 MPa). The first set of experiments studies the effects of miscible CO_2 and CO_2-WAG injection methods on both oil production and the decline in rock permeability of heterogeneous multi-layer reservoirs due to formation damage. The second set of experiments studies the effects of pore-throat microstructure on blockage and wettability during and after miscible CO_2 flooding.

Methodology

In the first set of core flooding experiments, three cores with significantly different permeabilities (one high, one medium and one low) were cut in half and put into two matched groups. The three cores from each group were arranged in parallel in a core-flooding assembly. One group of cores was subjected to miscible CO_2 flooding, while the other was subject to CO_2-WAG flooding. In each case, each core was placed in a core holder, and the core holders were arranged in parallel for contemporaneous core flooding, sharing the same input fluids, but having their output fluids monitored separately. The oil, gas and water production data from the two flooding methods were evaluated for residual oil distribution and permeability decline.

After the core flooding experiment was completed, the cores were cleaned twice by using n-heptane and toluene plus methanol, respectively. Asphaltene is soluble in solvents but not in alkanes (Wang et al., 2017). Consequently, the cores were first cleaned by using n-heptane. This procedure removes the remaining fluid in the cores after flooding, but not the asphaltenes or the inorganic precipitates. The cores were then dried and their porosity and gas permeability was measured. These are measurements which are affected by the presence of asphaltene deposits and inorganic precipitates resulting from CO_2–brine–rock interactions. The cores were then cleaned with toluene and methanol to remove the asphaltene, but leaving the inorganic precipitates in situ. The cores were dried once more and subjected to porosity and permeability measurement to obtain parameters which are only affected by the inorganic precipitates. In each measurement, the values we provide here are the arithmetic means of three physical measurements.

A second set of core flooding experiments was carried out in order to study the effect of pore size distribution and pore-throat microstructure on the distribution of blockages caused by both organic and inorganic precipitation, as well as changes in wettability caused by asphaltene precipitation. In these experiments, four cores with the very similar permeability value but very different typical pore throat size distributions were subjected to CO_2 flooding experiments. The cores were then cleaned using the same procedure that was described above. The cores were then re-saturated with water and oil in order to observe the size ranges of the pores and pore throats which had become blocked. This data was then used to interpret the measured difference in oil distribution before and after the flooding experiments.

The primary technique used to monitor changes to the rocks before, during and after core flooding was nuclear magnetic resonance spectroscopy (NMR) and constant-rate mercury intrusion (CRMI). These NMR measurements can detect the transverse relaxation of hydrogen nuclei of the fluids occupying the pores, providing a transversal relaxation time (T_2) spectrum. Variations in the T_2 spectrum reflect changes in the distribution of fluids in cores (Huang et al., 2019). In our measurements, NMR scanning was repeated three times to confirm the repeatability of the measurement. The mercury injection capillary pressure (MICP) obtained by CRMI was used to characterise the pore-throat structure of the cores. The wettability was assessed by Amott–Harvey wettability index both before and after flooding. For the wettability measurements, the core samples were aged in brine before each wettability test to eliminate the effect of oil saturation.

The core parameters for the samples used in the experiments are shown in Table 1, with calculated uncertainties in porosity measurements <0.4%, and uncertainties in permeability measurements of about 5%. The asphalt content of the oil used in the experiment was 1.32 wt.%, and the minimum miscibility pressure (MMP) of the CO_2-oil system was 16.8 MPa at 70°C. Consequently, the experimental pressure is considered to satisfy the condition for miscible flooding.

Table 1. Basic petrophysical properties of the core samples.

Core number	Length (cm)	Permeability (mD)	Porosity (%)	Flooding methods
Y1-1	3.12	0.59	10.68	CO_2 parallel
Y2-1	3.13	6.92	16.87	
Y3-1	3.14	64.1	19.85	
Y1-2	3.15	0.58	10.61	WAG parallel
Y2-2	3.10	6.78	16.69	
Y3-2	3.14	63.6	19.98	
H-1	5.11	0.713	14.62	CO_2 single
H-2	5.07	0.742	14.14	
H-3	5.09	0.769	13.62	
H-4	5.02	0.734	11.85	

The implementation of core-flooding experiments at reservoir conditions is complex and results in a significant non-zero uncertainty in the experimental measurements despite great efforts being made to reduce these experimental systematic and random errors. Such efforts have included averaging over multiple measurements whenever possible. The experimental porosity measurements presented in this work are very accurate, being less than ±0.5%. Permeability and fluid saturations are much more difficult to measure accurately, and are about ±5% and ±4%, respectively, in this work, which is still very good compared to other reservoir condition core-flooding measurements.

Comparison of CO_2 and CO_2-WAG Flooding

First let us consider the difference between carrying out a miscible CO_2 or a miscible CO_2-WAG core flooding at reservoir conditions on a parallel system of three different permeabilities; high, medium and low permeability cores coded by Y1, Y2 and Y3, respectively, as shown in Table 1..

For miscible CO_2 flooding, the distributions of residual oil in each core after flooding are shown in the top panel of Figure 1. It is clear that the oil in the medium and low permeability cores is hardly displaced by CO_2, and only a small part of the oil in the large core is produced. Consequently, the oil recovery of the multilayer system is determined by the high permeability core, which has the highest oil recovery factor (RF) and also the highest oil contribution percentage (OCP; the fraction of oil produced by each core expressed as a percentage of total system oil production). In our measurements the RF and OCP for the high permeability core were 54.6% and 91.37%, respectively. By contrast, the large amount of residual oil in the medium and low permeability cores results in a very low oil RF of the entire system, 27.64%. Both the heterogeneity of the system and the fingering effect lead to premature CO_2 breakthrough in the high permeability core (Alhamdan et al., 2012), after which injected CO_2 mainly flows through the cleared CO_2 channels in the high permeability core, exacerbating the differences in OCP between the high permeability core and the medium and low permeability cores and resulting in a low overall efficiency of CO_2 flooding.

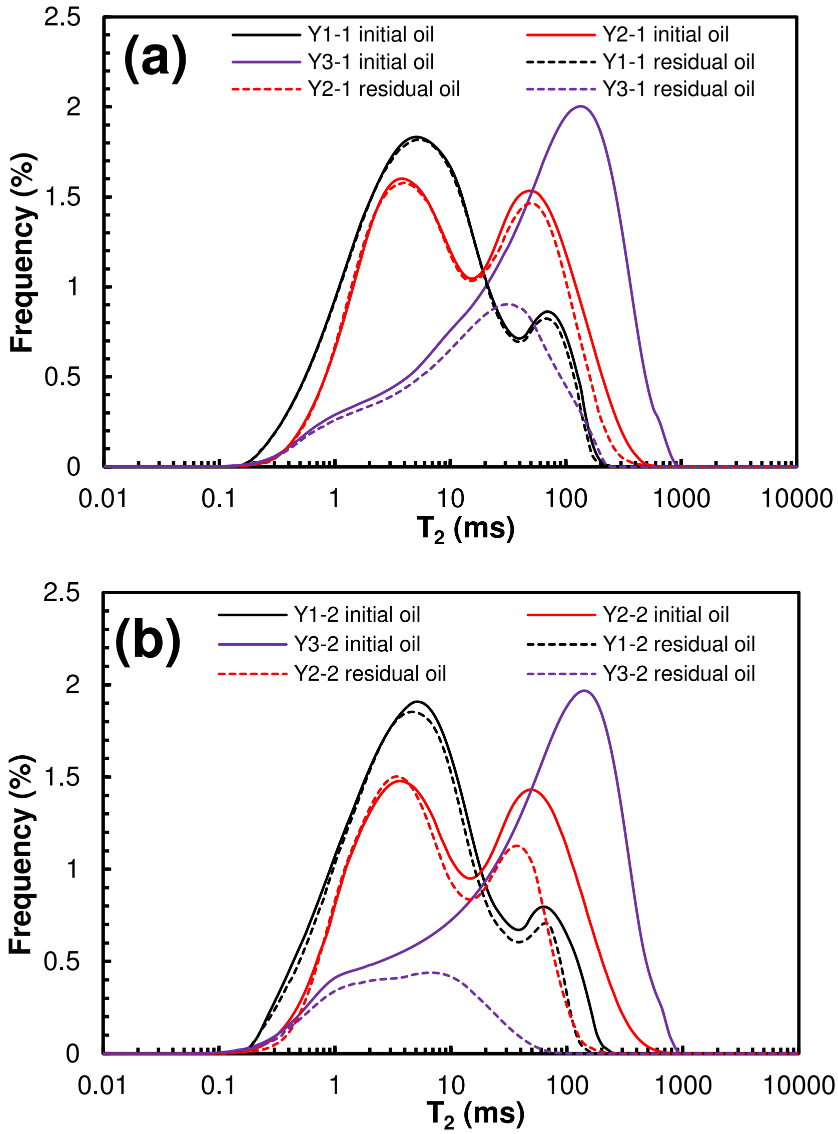

Figure 1. NMR T_2 spectra of oil distribution in cores after (a) CO_2 flooding, and (b) CO_2-WAG flooding. The solid curves of the top panel show the distribution of crude oil in the core of Y1-1, Y2-1 and Y3-1 before being displaced by CO_2 in parallel, and the dotted curves show the distribution of residual oil in cores after CO_2 flooding. The solid curves of the bottom panel show the distribution of crude oil in the core of Y1-2, Y2-2 and Y3-2 before being displaced by CO_2-WAG in parallel, and the dotted curves show the distribution of residual oil in cores after CO_2-WAG flooding.

By contrast, for CO_2-WAG flooding (the bottom panel of Figure 1), oil production is larger than that encountered after CO_2 flooding. In particular, the oil RF and OCP of the medium and low permeability cores are significantly improved, resulting in a higher oil RF of the entire system, 44.49%, with smaller differences between the OCP from each of the cores. In this regard it may be said that the operation of CO_2-WAG flooding is less sensitive to permeability heterogeneity in the model reservoir. It is worth noting that CO_2-WAG flooding was able to produce oil from smaller pores than that accessed by miscible CO_2 flooding, not only resulting in a higher oil recovery factor but also providing better permeabilities. Furthermore, for the CO_2-WAG flooding the CO_2 breakthrough was later compared to that for the miscible CO_2 flooding. In general, CO_2-WAG not only improves the oil displacement for each core irrespective of the permeability of that core, but also weakens the influence of multilayer system heterogeneity on the overall system oil recovery performance.

In summary, our results show that the miscible CO_2-WAG flooding is more efficient than using miscible CO_2 flooding alone, especially when applied to a system with heterogeneity in its permeability distribution. However, as we will see miscible CO_2-WAG flooding also has some disadvantages.

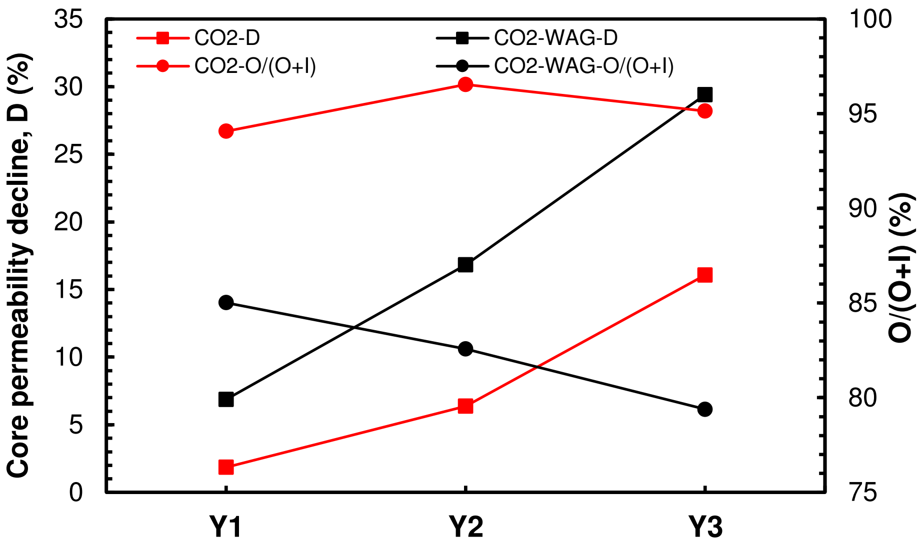

Figure 2. Overall permeability decline (D) of cores (left-hand x-axis) after miscible CO_2 and miscible CO_2-WAG flooding experiments, together with the percentage contribution of organic (asphaltene) precipitation to that decline (right-hand x-axis), quantified as the value O/(O+I), where O is the permeability decline associated with organic precipitation (asphaltene) and I is the permeability decline associated with inorganic interactions.

The permeability of all cores showed a decline after core flooding (Figure 2), with uncertainties about 5%. It is possible to say that in the same group of flooding experiments, the greater the initial permeability of the core, the greater the decrease of permeability. In all cases miscible CO_2-WAG flooding led to greater decreases in permeability than simple miscible CO_2 flooding by a factor of more than two. We also noted any decreases in the porosity for both core flooding processes. As expected, the decreases in porosity was much less dramatic than those for permeability for all cores and flooding techniques.

The significant decreases in permeability and slight decreases in porosity of cores are attributed to changes in the microstructure of pores and throats in rocks caused by organic deposition and CO_2-brine-rock interaction (Behbahani et al., 2014; Yu et al., 2012). When CO_2 is injected into cores, the asphaltene begins to precipitate from the crude oil, and then to aggregate to become asphaltene particles (Doryani et al., 2016). Moreover, metal carbonate precipitation also occurs due to changes in pH and the concentrations of metal ions (Gaus, 2010), and additional clay particles are released as a result of structural instability due to CO_2-brine-rock interactions (Iglauer et al., 2014). Consequently, blockage or partial blockage of flow pathways caused by these particles occurs. Such blockages may have little effect on rock porosity, but can reduce permeability significantly because permeability is a vector petrophysical property that is highly sensitive to the connectedness of the pore microstructure (Glover and Walker, 2008).

Since 3 cores with different permeability were flooded in parallel, most of the injected CO_2 flows through the high permeability core, which implies that the high permeability core will witness the passage of more mobile precipitant particles. Consequently, it would be expected that the high permeability core will be affected by more blockages at pore throats, resulting in a greater decrease in permeability for the high permeability cores. This, however, is not the whole story as those cores with lower permeability also have smaller pore throat sizes whose permeabilities are more sensitive to blockage. Consequently, the cores with lower permeability also undergo a clear decrease in permeability, even though the flow of CO_2 through them is much smaller, and the precipitation of both organic and inorganic pore throat blocking materials is subsequently lower.

The larger permeability decreases after CO_2-WAG flooding can be attributed to the higher injection pressure and the larger sweep volume of the injected fluid which occurs during this technique (Ahmadi et al., 2015). At higher pressures, concentrations of dissolved CO_2 in both the oil and water occupying the cores is higher, resulting in the fluid–fluid and fluid–rock interactions being more complete. The larger sweep volume associated with the CO_2-WAG flooding ensures that precipitation and particle blockages occur throughout a greater number of pores and pore throats in the rock including smaller pores and pore throats.

The permeability decline due to asphaltene precipitation during the miscible CO_2 flooding is dominant, at around 95% (as shown in Figure 2). Since the connate water is both distributed in the smallest pores and covers the surfaces of the larger pores in the form of a water film (Xiao et al., 2019), the injected CO_2 does not come into contact simultaneously with both brine and minerals, and hence CO_2-brine-rock interactions have little effect on the permeability decline. In the CO_2-WAG flooding, the permeability decline caused by CO_2-brine-rock interactions is significantly higher than that in miscible

CO_2 flooding, and as the initial permeability increases, the ratio of the permeability decline caused by asphaltene precipitation to the total permeability decline decreases. This is because more oil is displaced from the cores during the CO_2-WAG flooding, especially in cores with high permeability. Consequently, for CO_2-WAG flooding, the pervasive distribution of brine and CO_2 during the flooding process makes brine and CO_2 more likely to be in contact with minerals, and enhances CO_2-brine-rock interactions. However, despite this, more oil can be in contact with CO_2 and displaced during CO_2-WAG flooding. Hence more asphaltene is trapped in the cores, resulting more serious asphaltene blockage than that in the corresponding cores during CO_2 flooding.

Effect of Pore and Pore-throat Microstructure in Miscible CO_2 Flooding

In this section we consider the differences in miscible CO_2 flooding for four reservoir rock samples (H1 to H4) with the same permeability but very different pore microstructures in order to understand the processes leading to better oil recovery and formation damage reduction by organic and inorganic precipitates.

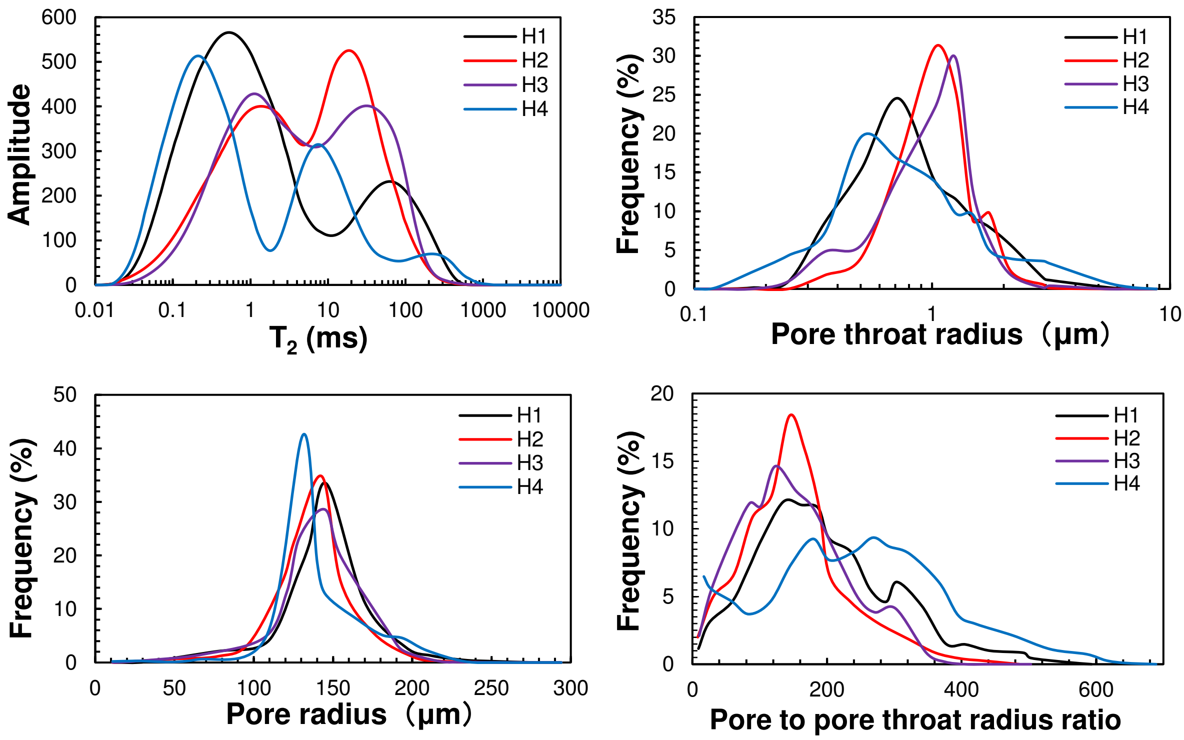

Figure 3. NMR and CRMI results before experiments. The upper left panel shows the T_2 spectrum of four cores in fully saturated brine before experiments obtained by NMR tests, reflecting the pore size distribution of the four cores. The other three graphs are the distributions of throat radius, pore radius and the pore throat ratio before experiments according to the results of CRMI tests.

The predominant type of T_2 distribution in ultra-low permeability rocks is bimodal (Gao et al., 2015). Figure 3 shows NMR and MICP results for each of four reservoir rock samples which share the same permeability but have significantly different pore and pore throat sizes and structures. In each case the permeability of the sample initially was 0.7395+0.0295-0.0265% (arithmetic mean and +/– range).

The pore throats connecting the pores play a dominant role in influencing the permeability of cores, while the pores themselves are the places where the reservoir fluids are stored. The results of our MICP measurements show that the throat distributions of H2 and H3 have peaks which are narrower and occur at larger values of pore throat size than for the other two cores. This implies that these two cores have a considerable proportion of large pore throats. By contrast, the pore throat distributions of samples H1 and H4 are spread out more and peak at a lower pore throat sizes. Indeed, for these samples there are a few pore throats in the cores that are larger than 2 μm in size, which is lower than the pore throat threshold for gas flow used in the calculation of potential porosity. The MICP data also shows that there is no significant difference in the pore distribution of the four cores, but this does not imply that the four cores have the same pore volume. The fact that all four samples share the same approximate permeability allows us to infer that samples H2 and H3, though having larger pore throat sizes, have pores which are less well-connected than samples H1 and H4. In addition, the distributions of pore-throat ratio also imply that H1 and H4 have strong heterogeneity in pore-throat microstructure, and H3 has the best pore-throat microstructure.

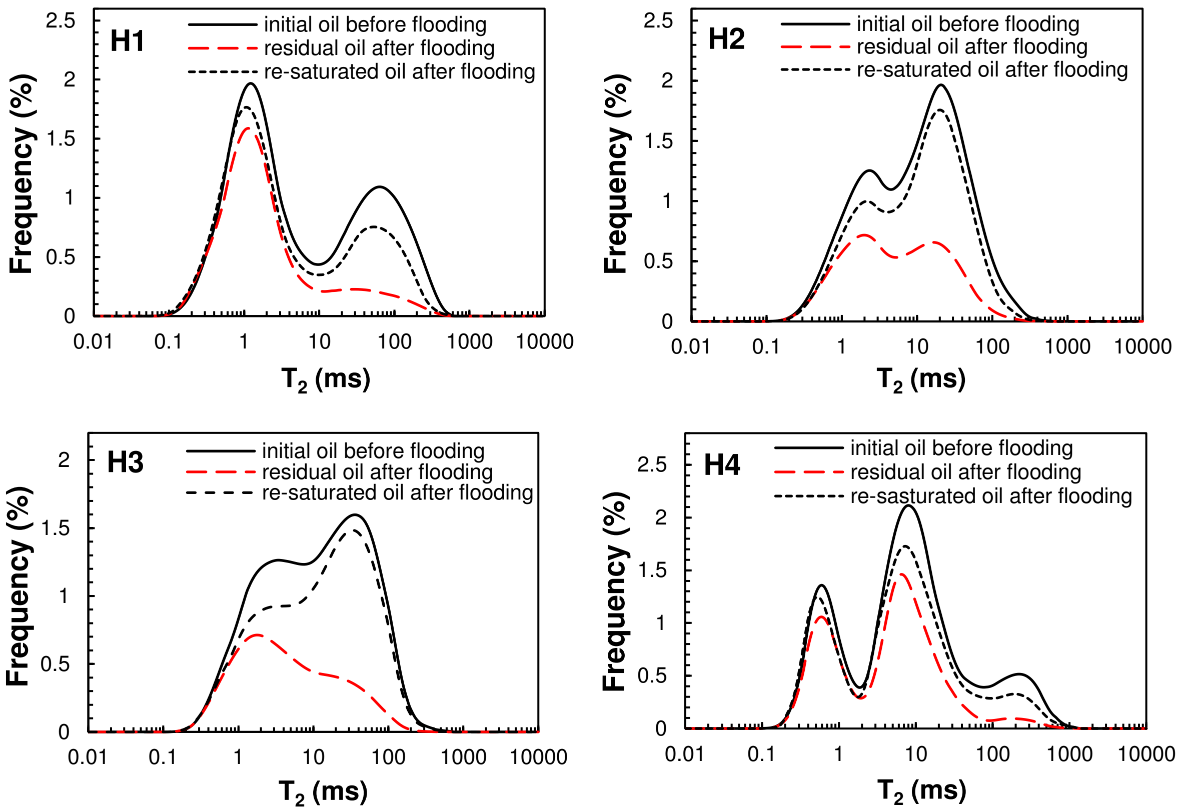

Figure 4. NMR T_2 spectrum of oil distribution in cores. The solid curves show the distribution of crude oil in the four cores before CO_2 flooding, and the red dotted curves show the distribution of residual oil after CO_2 flooding. The cores were cleaned and only the asphaltene precipitate remains in the pores after CO_2 flooding, then the cores were re-saturated with brine and crude oil, and the black dotted curves show the distribution of re-saturated crude oil.

The T_2 spectra given in Figure 4 show the distribution of initial oil before flooding, residual oil and re-saturated oil after flooding. In interpreting these diagrams, small values of T_2 represent small pores in the rock, while larger values of T_2 represent larger pores. This figure shows that the residual oil of H2 and H3 is less than for H1 and H4. It is especially interesting that only a small portion of the oil in the small pores of H1 and H4 is driven out (the data for which T_2<5 ms). The variation in oil saturation (S_{ov}, where $S_{ov} = S_{ob} - S_{oa}$, and S_{ob} is the initial oil saturation before flooding, and S_{oa} is the oil re-saturation after flooding) represents the degree of change in petrophysical properties after flooding. Although the total S_{ov} values of H1and H4 are only slightly larger than those of H2 and H3, the S_{ov} is much smaller for the oil produced from small pores, but much larger for oil produced from the large pores, especially in H1 and H4.

Oil re-saturation after flooding is affected by two factors; (i) blockage of the pore throats, and (ii) changes to the wettability of cores. When pore throats connecting pores are blocked, some pores in the rock are not re-saturated with oil. Consequently, the signal amplitude of the large pores on the right side of the T_2 spectrum shows significant decline. However, the asphaltene precipitate adsorbs to the surface of the pores, which reduces the wettability index of the rocks, making the asphaltene precipitated rocks more oil wet. This process of progressive oil wettening aids oil re-saturation. Consequently, the smaller S_{ov} in the small pores of H1 and H4 is caused by little oil production. Although both large and small pores produce oil in H2 and H3, the structure of the small pores and associated pore throats is more likely to be modified by asphaltene precipitation. Moreover, H2 and H3 undergo large changes in wettability, which may also be the reason for a higher measured oil re-saturation.

The degree of blockage at throats was found to determine directly the extent of the decrease in gas permeability in these miscible CO_2 flooding experiments. The S_{ov} values of the four cores are close, and the values in throats of small pores in the left of the spectra of H1 and H4 is relatively high, but the permeability of H2 and H3 decreases significantly less than H1 and H4 after flooding (the top panel of Figure 5). This may be attributed to the pore-throat microstructure with strong heterogeneity of H1 and H4. Here the main seepage path is preferentially blocked during flooding process, which represents serious damage to the permeability the reservoir rock, and the changes in permeability of cores with smaller throat are more sensitive to blockage. In addition, although the pore throats of H2 and H3 are partially blocked and the permeability is reduced, it seems that the oil re-saturation of the larger pores is not greatly affected, possibly due to the homogeneity of the pore throat microstructure.

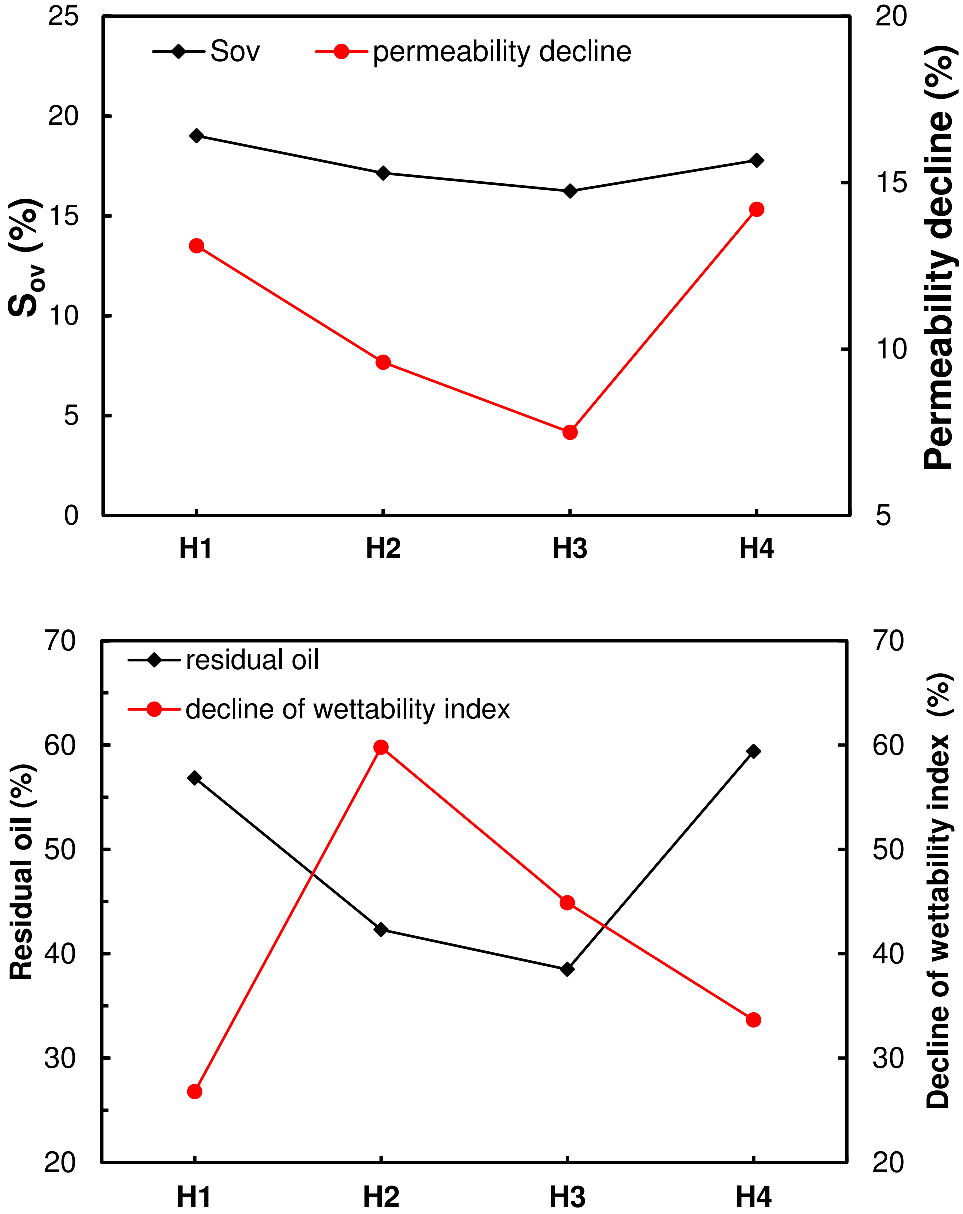

Figure 5. Top panel – the black solid line represents the variation in oil saturation (S_{ov}) before and after flooding, and the red solid line represents permeability decline of four cores after CO_2 flooding; Bottom panel - the black solid line represents the distribution of residual oil, and the red solid line represents the variation of wettability of four cores after CO_2 flooding. The y-axis uncertainties are <±4%.

The degree of change in wettability is negatively correlated with the percentage fraction of residual oil, as shown in the bottom panel of Figure 5. It has already been noted that residual oil distribution is affected by the pore-throat microstructure (Chatzis et al., 1988). In H2 and H3, the sweep volume of CO_2 is larger, which implies that oil is displaced from more pores on whose pore surfaces more asphaltene precipitation adsorption occurs, resulting in the rock becoming more oil wet, and hence able to imbibe more oil once again; a propensity recently noted by Fager et al. (2019) in lattice Boltzmann modelling of pore scale rock models. More oil production means more asphaltene precipitation, but leading to a smaller permeability decline, which again proves that the type of pore-throat microstructure of H2 and H3, especially H3, is more resistant to damage to rock properties by asphaltene precipitation.

In addition, it is also necessary to take into consideration vapour/liquid equilibrium in confined pores. Liu et al. (2018) have recently shown that the pore size and heterogeneity in the pore microstructure can affect vapour/liquid equilibria locally, leading to changes in the fluid, with a Peng-Robinson Equation of State study implemented with engineering Density-Functional Theory. Such local disequilibria could perturb the flood efficiency and also lead to preferential local conditions for asphaltene precipitation.

Conclusions

Studies of miscible CO_2 and CO_2-WAG flooding for layered heterogeneous systems with different permeabilities and of miscible CO_2 flooding for samples of the same permeability but different pore and pore throat structures and varying wettability, have shown complex behaviours with regard to the efficiency with which oil can be produced and the sensitivity of the reservoir systems to permeability damage resulting from organic asphaltene and inorganic precipitates.

It has been found that during and after miscible CO_2 flooding oil production from the multi-layer reservoir occurs almost exclusively from the high-permeability layer, with a large amount of residual oil being left unproduced in the lower permeability layers. By contrast, the CO_2-WAG flooding provides a higher oil displacement efficiency and an ability to reduce the impact of interlayer heterogeneity, improving the contribution of oil production in lower permeability layers. Miscible CO_2 flooding caused formation damage in each of the samples representing the layered system, leading to reductions in permeability, and was particularly strong in the high-permeability rock. The reductions in permeability were caused mainly by asphaltene precipitation. Formation damage leading to permeability reductions resulting from asphaltene precipitation was even greater during and after CO_2-WAG flooding, affecting each layer of the model. This may be a key consideration in the choice of whether or not to use CO_2-WAG flooding in some reservoir developments. While asphaltene precipitation was the principal cause of formation damage and permeability reduction, permeability decline caused by CO_2–brine–rock interactions producing inorganic precipitates was also noted in the experimental results, and occurred more in the high permeability rocks during CO_2-WAG flooding.

Rocks with strong heterogeneity in their pore-throat microstructure were found to retain more residual oil after CO_2 flooding, especially in small pores. However, the pore throats of these cores are can be blocked more effectively and extensively than larger pore throats, leading to a significant decrease in permeability in heterogeneous reservoir rocks. The permeability of cores with homogeneous pore-throat microstructures is less sensitive to asphaltene precipitation, and changes in wettability to a more oil-wet state are greater. The water-wettability of the rocks becomes weaker due to asphaltene precipitation, and the variation range of wettability is negatively correlated with the residual oil.

Acknowledgments

We would like to thank Yang Shenglai and Qian Kun for their work on the experiments. This research is supported by National Natural Science Foundation of China, “Study on the physical basis of seepage in ultra-deep clastic reservoirs” (51774300), and “Key technologies for CO_2 flooding and storage” of the 13th Five-Year National Major Science and Technology Project (2016ZX05016006-004).

Data and materials availability

The data associated with this research are confidential and cannot be released.

References

Al-Maamari, R.S. and Buckley, J.S., 2003. Asphaltene precipitation and alteration of wetting: the potential for wettability changes during oil production. SPE Reservoir Evaluation & Engineering, 6(04), 210-214.

Al-Mahrooqi, S.H., Grattoni, C.A., Moss, A.K. and Jing, X.D., 2003. An investigation of the effect of wettability on NMR characteristics of sandstone rock and fluid systems. Journal of Petroleum Science and Engineering, 39(3-4), 389-398.

Alhamdan, M.R., Cinar, Y., Suicmez, V.S. and Dindoruk, B., 2012. Experimental and numerical study of compositional two-phase displacements in layered porous media. Journal of Petroleum Science and Engineering, 98, 107-121.

Ahmadi, Y., Eshraghi, S.E., Bahrami, P., Hasanbeygi, M., Kazemzadeh, Y. and Vahedian, A., 2015. Comprehensive Water–Alternating-Gas (WAG) injection study to evaluate the most effective method based on heavy oil recovery and asphaltene precipitation tests. Journal of Petroleum Science and Engineering, 133, 123-129.

Behbahani, T.J., Ghotbi, C., Taghikhani, V. and Shahrabadi, A., 2014. Investigation of asphaltene adsorption in sandstone core sample during CO_2 injection: Experimental and modified modeling. Fuel, 133, 63-72.

Chatzis, I., Kuntamukkula, M.S. and Morrow, N.R., 1988. Effect of capillary number on the microstructure of residual oil in strongly water-wet sandstones. SPE Reservoir Engineering, 3(3), 902-912.

Doryani, H., Malayeri, M.R. and Riazi, M., 2016. Visualization of asphaltene precipitation and deposition in a uniformly patterned glass micromodel. Fuel, 182, pp.613-622.

Fager, A., Crouse, B., Sun, G., Xu, R., & Freed, D., 2019. Evaluation of Directly Simulated WAG Hysteresis at Pore Scale and its Effect on Injectivity Index. Society of Petroleum Engineers. Proceedings SPE Offshore Europe Conference and Exhibition 3-6 September 2019, Aberdeen, UK, doi:10.2118/195734-MS

Gao, H. and Li, H., 2015. Determination of movable fluid percentage and movable fluid porosity in ultra-low permeability sandstone using nuclear magnetic resonance (NMR) technique. Journal of Petroleum Science and Engineering, 133, 258-267.

Gaus, I., 2010. Role and impact of CO_2–rock interactions during CO_2 storage in sedimentary rocks. International Journal of Greenhouse Gas Control, 4, 73–89.

Glover, P.W.J. and Walker, E., 2008. Grain-size to effective pore-size transformation derived from electrokinetic theory. Geophysics, 74(1), pp.E17-E29

Han, L., Gu, Y., 2014. Optimization of miscible CO_2 water-alternating-gas injection in the Bakken formation. Energy & Fuels, 28(11), 6811-6819.

Huang, X., Li, T., Gao, H., Zhao, J. and Wang, C., 2019. Comparison of SO_2 with CO_2 for recovering shale resources using low-field nuclear magnetic resonance. Fuel, 245, pp.563-569.

Iglauer, S., Sarmadivaleh, M., Al-Yaseri, A. and Lebedev, M., 2014. Permeability evolution in sandstone due to injection of CO2-saturated brine or supercritical CO_2 at reservoir conditions. Energy Procedia, 63, pp.3051-3059.

Kong, S., Huang, X., Li, K. and Song, X., 2019. Adsorption/desorption isotherms of CH_4 and C_2H_6 on typical shale samples. Fuel, 255, 115632.

Lei, H., Yang, S., Zu, L., Wang, Z. and Li, Y., 2016. Oil recovery performance and CO_2 storage potential of CO_2 water-alternating-gas injection after continuous CO_2 injection in a multilayer formation. Energy & Fuels, 30(11), pp.8922-8931.

Li, J., Liu, Y., Gao, Y., Chen, B., Meng, F. and Xu, H., 2018. Effects of microscopic pore structure heterogeneity on the distribution and morphology of remaining oil. Petroleum Exploration and Development, 45(6), pp.1112-1122.

Liu, Y., Jin, Z., & Li, H.A., 2018. Comparison of Peng-Robinson equation of state with capillary pressure model with engineering density-functional theory in describing the phase behavior of confined hydrocarbons. Journal of the Society of Petroleum Engineers, 187405-PA. doi:10.2118/187405-PA

Wang, Q., Yang, S., Han, H., Wang, L., Qian, K. and Pang, J., 2019. Experimental Investigation on the Effects of CO_2 Displacement Methods on Petrophysical Property Changes of Ultra-Low Permeability Sandstone Reservoirs near Injection Wells. Energies, 12(2), 327.

Wang, Z., Yang, S., Lei, H., Yang, M., Li, L. and Yang, S, 2017. Oil recovery performance and permeability reduction mechanisms in miscible CO_2 water-alternative-gas (WAG) injection after continuous CO_2 injection: An experimental investigation and modeling approach. Journal of Petroleum Science and Engineering, 150, 376-385.

Xiao, P., Lv, C., Wang, R., Cui, M., Xu, Q., Hu, Q. and Hu, W., 2019. Laboratory study heterogeneity impact on microscopic residual oil distribution in tight sandstone cores during CO_2 immiscible flooding. Energy Sources, Part A: Recovery, Utilization, and Environmental Effects, 1-11.

Yu, Z., Liu, L., Yang, S., Li, S., & Yang, Y., 2012. An experimental study of CO_2–brine–rock interaction at in situ pressure–temperature reservoir conditions. Chemical Geology, 326, 88-101.

Zou, Y., Li, S., Ma, X., Zhang, S., Li, N. and Chen, M, 2018. Effects of CO_2–brine–rock interaction on porosity/permeability and mechanical properties during supercritical-CO_2 fracturing in shale reservoirs. Journal of Natural Gas Science and Engineering, 49, 157-168.